Earth and Planetary Science Letters 373 (2013) 75–82

Contents lists available at SciVerse ScienceDirect

Earth and Planetary Science Letters

journal homepage: www.elsevier.com/locate/epsl

Redox state during core formation on asteroid 4-Vesta

Emily A. Pringle [a,*], Paul S. Savage [a], James Badro [b], Jean-Alix Barrat [c], Frédéric Moynier [a]

[a] Department of Earth Planetary Sciences, McDonnell Center for the Space Sciences, Washington University in St. Louis, One Brookings Drive, St. Louis, MO 63130, USA
[b] Institut de Physique du Globe de Paris, 1 rue Jussieu, 75005 Paris, France
[c] Université Européenne de Bretagne, Université de Brest, CNRS UMR 6538 (Domaines Océaniques), I.U.E.M., Place Nicolas Copernic, 29280 Plouzané Cedex, France

ARTICLE INFO

Article history:
Received 1 February 2013
Received in revised form
8 April 2013
Accepted 10 April 2013
Editor: B. Marty
Available online 14 May 2013

Keywords:
silicon isotopes
eucrites
Vesta
core formation

ABSTRACT

Core formation is the main differentiation event in the history of a planet. However, the chemical composition of planetary cores and the physicochemical conditions prevailing during core formation remain poorly understood. The asteroid 4-Vesta is the smallest extant planetary body known to have differentiated a metallic core. Howardite, Eucrite, Diogenite (HED) meteorites, which are thought to sample 4-Vesta, provide us with an opportunity to study core formation in planetary embryos.

Partitioning of elements between the core and mantle of a planet fractionates their isotopes according to formation conditions. One such element, silicon, shows large isotopic fractionation between metal and silicate, and its partitioning into a metallic core is only possible under very distinctive conditions of pressure, oxygen fugacity and temperature. Therefore, the silicon isotope system is a powerful tracer with which to study core formation in planetary bodies. Here we show through high-precision measurement of Si stable isotopes that HED meteorites are significantly enriched in the heavier isotopes compared to chondrites. This is consistent with the core of 4-Vesta containing at least 1 wt% of Si, which in turn suggests that 4-Vesta's differentiation occurred under more reducing conditions (ΔIW~−4) than those previously suggested from analysis of the distribution of moderately siderophile elements in HEDs.

1. Introduction

Knowledge of the chemical and isotopic compositions of a planet's core is fundamental to understanding the conditions (e.g. oxidation state, pressure, and temperature) prevailing during core/mantle differentiation. In the absence of direct sampling, the approach used to determine core composition has been to compare the composition of undifferentiated primitive meteorites (chondrites) to samples representative of mantle material (e.g. Allègre et al., 1995; McDonough, 2003; Georg et al., 2007; Moynier et al., 2011), as well as to measure elemental partitioning between metal and silicate phases under different physical conditions (Wade and Wood, 2005; Ricolleau et al., 2011; Siebert et al., 2012).

In particular, silicon (Si) metal–silicate partitioning is very sensitive to temperature, oxygen fugacity and pressure. It becomes more siderophile with increasing temperature and pressure and with decreasing oxygen fugacity (Kilburn and Wood, 1997; Gessmann et al., 2001; Wade and Wood, 2005; Ricolleau et al., 2011; Siebert et al., 2012). Furthermore, partitioning experiments (Shahar et al., 2009, 2011; Kempl et al., 2013), direct measurement in meteorites (Ziegler et al., 2010) and *ab initio* calculations (Georg et al., 2007) consistently show that, at equilibrium, metallic Si is preferentially enriched in light Si isotopes compared to silicates. A small but measureable heavy Si isotopic enrichment in the Bulk Silicate Earth (BSE) compared to chondrites has been interpreted as evidence for the incorporation of ~4–7 wt% Si into the Earth's core (Georg et al., 2007; Fitoussi et al., 2009; Savage et al., 2010; Armytage et al., 2011), which is in good agreement with seismic observations and elasticity models (Birch, 1964; Badro et al., 2007; Antonangeli et al., 2010).

4-Vesta is the second largest main-belt asteroid and is the only known intact asteroid thought to have differentiated a metallic core (Russell et al., 2012). The Howardite, Eucrite, Diogenite (HED) meteorites form a class of achondrites that, based on spectroscopic data, are believed to sample the silicate portion of 4-Vesta (see De Sanctis et al. (2012), for a recent review). In addition, HEDs are among the oldest differentiated material in the Solar System, with crystallization ages of ~1–3 Myr after CAI formation (Trinquier et al., 2008). Therefore, HED meteorites provide us with a unique opportunity to study the early stages of core formation in the Solar System.

The study of Si isotopes in HED meteorites has the potential to provide an estimate of the abundance of Si in 4-Vesta's core.

* Corresponding author. Tel.: +1 3149357292.
E-mail address: eapringle@levee.wustl.edu (E.A. Pringle).

0012-821X/$ - see front matter © 2013 Elsevier B.V. All rights reserved.
http://dx.doi.org/10.1016/j.epsl.2013.04.012

The sizes of 4-Vesta and its core are now well known due to the results from NASA's recent Dawn mission (Russell et al., 2012), so a precise range of pressures and temperatures for the core boundary metal–silicate equilibrium can be estimated. Therefore, the abundance of Si in 4-Vesta's core can be used to calculate the oxygen fugacity prevailing during core formation. To date, however, there are very few Si isotopic analyses of HED samples (Fitoussi et al., 2009; Chakrabarti and Jacobsen, 2010; Armytage et al., 2011; Zambardi, 2011). On average, these studies report a hint of enrichment in the heavier Si isotopes in HEDs compared to chondrites, but such variations are within analytical error, and on this basis no firm conclusions on the composition of 4-Vesta's core can be made.

Here we use an innovative analytical approach to report high-precision Si isotope data in HEDs, Martian meteorites and chondrites. We use the Si isotopic offset between HEDs and chondrites to quantify the abundance of Si in the core of 4-Vesta. Using models of Si partitioning between metal and silicate, we calculate the redox conditions during core formation on 4-Vesta.

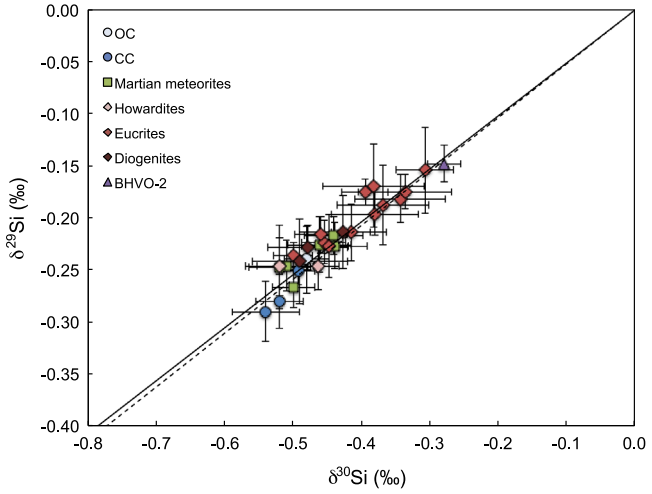

Fig. 1. Three-isotope plot of δ^{29}Si vs. δ^{30}Si. All data fall within error (± 2 se) of the calculated mass-dependent equilibrium (dashed line, slope 0.5178) and kinetic (solid line, slope 0.5092) fractionation lines.

2. Samples and analytical methods

Eucrites are basaltic rocks that display magmatic textures and chemical compositions indicating formation as lava flows or intrusions. Diogenites are orthopyroxene-rich cumulates that formed in a plutonic environment. Commonly, diogenites and eucrites also record impact events, and therefore are usually breccias consisting of a mixture of crystal debris and rock fragments. Howardites are complex breccias made of a mixture of diogenitic and eucritic debris (Barrat et al., 2010). In this study we have measured the Si isotopic composition of two howardites, nine eucrites, and three diogenites. Six Martian meteorites were also studied: three nakhlites, two shergotites, and the orthopyroxenite Allan Hills 84001. In addition, we have analyzed the carbonaceous chondrites Cold Bokkeveld (CM2) and Allende (CV3).

The analytical methods used in this manuscript are similar to those described in our previous Si isotope paper, for which extensive tests were performed (Savage and Moynier, 2013). Samples were dissolved following the HF-free alkali fusion technique described by Georg et al. (2006). Approximately 0.5 g of meteorite was crushed in an agate mortar to ensure sample homogeneity, of which ~10 mg of powdered sample and ~200 mg analytical grade NaOH flux were weighed into a silver crucible made of 99.99% pure Ag sheet and heated in a muffle furnace at 720 °C for 12 min. After cooling slightly, the crucible was immersed in 20 mL of MilliQ H_2O in a PTFE vial and left to equilibrate overnight. Following equilibration, the capped PTFE vial was placed in an ultrasonic bath for 60 min to agitate the fusion cake. The sample solution was then transferred into a pre-cleaned polypropylene bottle, diluted with MilliQ H_2O to yield a final solution concentration of ~20 ppm Si and acidified to 1% v/v HNO_3.

All samples and standards were purified through an ion exchange chromatography procedure using BioRad AG50 X-12 (200–400 mesh) cation exchange resin, also described in Georg et al. (2006). Because Si exists in solution as non-ionic or anionic species at low pH, it is not retained by the resin and is therefore effectively separated from cationic matrix elements and quantitatively eluted immediately after loading using MilliQ H_2O. Sample column loads were calculated to result in a final Si concentration of 3.0 ppm following column chemistry. After purification, each sample was acidified to 1% v/v HNO_3.

Silicon isotope measurements were made on a Thermo Scientific Neptune Plus Multi-Collector Inductively-Coupled-Plasma Mass-Spectrometer (MC-ICP-MS) at Washington University in St. Louis, operating at medium resolution. Isotope measurements were calculated using standard-sample bracketing to correct for any instrumental drift over time. The quartz sand standard NBS28 (NIST RM8546) and the carbonaceous chondrites Cold Bokkeveld and Allende were all used as bracketing standards to obtain measurements during separate analytical sessions. Silicon isotope variations are defined in per mil units (‰) using the delta notation relative to a bracketing standard:

$$\delta^x Si = \left[\frac{(^xSi/^{28}Si)_{sample}}{(^xSi/^{28}Si)_{standard}} - 1\right] \times 1000$$

where $x=29$ or 30. In a δ^{29}Si vs. δ^{30}Si plot (Fig. 1), all of the samples bracketed by NBS28 measured in this study fall within error of the calculated mass-dependent equilibrium (slope 0.5178) and kinetic (slope 0.5092) fractionation lines, and to date no Si isotope anomalies have been detected in bulk meteorites. Therefore, the remainder of the text discusses the Si isotopic data in terms of δ^{30}Si.

3. Results

Silicon isotope data relative to NBS28 as the bracketing standard are reported in Table 1 and Fig. 2. Both the 2 standard deviation (2 sd) and 2 standard error (2 se) are provided in Table 1; for comparison with previous Si isotope literature data the errors discussed throughout the text are 2 se unless otherwise specified.

To assess the reproducibility of the data, the isotopic composition of the well-characterized terrestrial basalt, BHVO-2, was measured during each analytical session. Our BHVO-2 value of $\delta^{30}Si = -0.28 \pm 0.02$‰ is in very good agreement with previously published values (e.g. Abraham et al., 2008; Savage et al., 2010; Armytage et al., 2011). The carbonaceous chondrite Allende was measured as a secondary check for data accuracy during most analytical sessions throughout this study, and the average value ($\delta^{30}Si = -0.49 \pm 0.02$‰) is in agreement with recent literature data (Armytage et al., 2011; Savage and Moynier, 2013). The Si isotope average of the carbonaceous chondrites reported in Table 1 ($\delta^{30}Si = -0.52 \pm 0.03$‰) is consistent with the average value previously reported by Armytage et al. (2011); ($\delta^{30}Si = -0.48 \pm 0.04$‰). Finally, the average Si isotopic composition of the Martian meteorites measured in this study ($\delta^{30}Si = -0.48 \pm 0.03$‰) is indistinguishable from chondrites and is consistent with previous

Table 1
Silicon isotope data for terrestrial standard and meteorite samples relative to NBS28 as the bracketing standard.

Sample	Group	δ^{29}Si	2 sd[a]	2 se[b]	δ^{30}Si	2 sd	2 se	*n*[c]
BHVO-2	Terrestrial basalt	−0.15	0.09	0.02	−0.28	0.12	0.02	26
Ordinary chondrites								
Parnallee[d]	LL3.6	−0.24	0.08	0.03	−0.48	0.08	0.03	6
Carbonaceous chondrites								
Allende	CV3	−0.25	0.06	0.01	−0.49	0.11	0.02	20
Cold Bokkeveld[d]	CM2	−0.28	0.09	0.03	−0.52	0.12	0.03	12
Murray[d]	CM2	−0.29	0.07	0.03	−0.54	0.12	0.05	6
Average-carbonaceous chondrites		**−0.27**	**0.04**	**0.02**	**−0.52**	**0.05**	**0.03**	**3**
Martian meteorites								
Sayh al Uhaymir 008	Shergottite	−0.25	0.06	0.02	−0.51	0.11	0.04	7
Los Angeles	Shergottite	−0.27	0.05	0.02	−0.50	0.08	0.03	6
Miller Range 03346	Nakhlite	−0.25	0.07	0.03	−0.52	0.11	0.05	6
Lafayette	Nakhlite	−0.23	0.07	0.03	−0.46	0.11	0.05	6
Nakhla	Nakhlite	−0.23	0.05	0.02	−0.44	0.12	0.05	6
Allan Hills 84001	Orthopyroxenite	−0.22	0.04	0.02	−0.44	0.11	0.04	6
Average-Martian meteorites		**−0.24**	**0.04**	**0.02**	**−0.48**	**0.07**	**0.03**	**6**
HED meteorites								
Kapoeta	Howardite	−0.25	0.06	0.02	−0.46	0.07	0.03	6
Frankfort	Howardite	−0.25	0.09	0.04	−0.52	0.11	0.05	5
Average-howardites		**−0.25**	**0.00**	**0.00**	**−0.49**	**0.08**	**0.06**	**2**
Serra de Magé	Eucrite (cumulate)	−0.21	0.07	0.03	−0.42	0.07	0.03	6
Petersburg	Eucrite (polymict)	−0.18	0.06	0.02	−0.34	0.16	0.07	6
Cachari #1	Eucrite-MG[e] (monomict)	−0.17	0.04	0.02	−0.34	0.17	0.07	6
Cachari #2	Eucrite-MG[e] (monomict)	−0.18	0.03	0.01	−0.39	0.09	0.03	7
Cachari mean		−0.17	0.00	0.00	−0.37	0.08	0.06	2
Camel Donga	Eucrite-MG[e] (monomict)	−0.20	0.05	0.02	−0.38	0.16	0.06	6
Jonzac	Eucrite-MG[e] (monomict)	−0.17	0.10	0.04	−0.38	0.18	0.07	6
Juvinas	Eucrite-MG[e] (monomict)	−0.24	0.03	0.01	−0.50	0.06	0.03	5
Bouvante #1	Eucrite-ST[f] (monomict)	−0.15	0.10	0.04	−0.31	0.10	0.04	6
Bouvante #2	Eucrite-ST[f] (monomict)	−0.22	0.06	0.02	−0.45	0.08	0.03	7
Bouvante mean		−0.19	0.10	0.07	−0.38	0.21	0.15	2
Stannern #1	Eucrite-ST[f] (monomict)	−0.19	0.09	0.04	−0.37	0.16	0.07	6
Stannern #2	Eucrite-ST[f] (monimict)	−0.23	0.07	0.03	−0.45	0.06	0.03	5
Stannern mean		−0.21	0.06	0.04	−0.41	0.11	0.08	2
Pomozdino	Eucrite-ST[f] (cumulate)	−0.22	0.04	0.02	−0.46	0.09	0.04	5
Average-eucrites		**−0.20**	**0.04**	**0.01**	**−0.40**	**0.10**	**0.03**	**9**
Aioun el Atrouss	Diogenite (polymict)	−0.21	0.09	0.04	−0.43	0.16	0.06	6
Tatahouine	Diogenite	−0.24	0.10	0.04	−0.49	0.17	0.07	6
Shalka	Diogenite	−0.23	0.05	0.02	−0.48	0.14	0.06	6
Average-diogenites		**−0.23**	**0.03**	**0.02**	**−0.47**	**0.07**	**0.04**	**3**
Average-All HED		**−0.21**	**0.05**	**0.01**	**−0.43**	**0.11**	**0.03**	**14**
Average-eucrites and diogenites		**−0.21**	**0.05**	**0.01**	**−0.42**	**0.10**	**0.03**	**12**

[a] 2 sd = 2 × standard deviation.
[b] 2 se = 2 × standard deviation/$\sqrt{n}$.
[c] n = number of measurements.
[d] Data from Savage and Moynier (2013).
[e] Eucrite (MG) = main group eucrite.
[f] Eucrite (ST) = Stannern-trend eucrite.

studies (Armytage et al., 2011). The overall excellent agreement between our data and previous literature data indicates that our methods are robust and provide an accurate analysis of Si isotope composition.

The average isotopic composition of all HED meteorites measured is δ^{30}Si = -0.43 ± 0.03‰. It has been recently noted that howardites contain chondrite debris (e.g. Janots et al., 2012); therefore, although it does not significantly affect the value, howardites have here been excluded from the HED meteorite average taken as representative of the silicate portion of the HED parent body (henceforth denoted δ^{30}Si (BSV); δ^{30}Si (BSV) = -0.42 ± 0.03‰). The δ^{30}Si of eucrites and diogenites reported here range from −0.34‰ to −0.50‰ and −0.43‰ to −0.49‰, respectively. Although, on average, eucrites are heavier with respect to Si isotopes than diogenites, both sample sets are isotopically heavier than chondrites, and the smaller range in the diogenite data may be due to the smaller number of samples (n = 3) compared to eucrites (n = 9).

In order to directly measure the difference in Si isotopic composition between HED meteorites and chondrites, the carbonaceous chondrites Cold Bokkeveld and Allende were each used as bracketing standards in several separate measurement sessions; these data are denoted $\delta^{30}Si_{CB}$ and $\delta^{30}Si_{Allende}$, respectively, and are presented in Table 2 and Fig. 3. This direct comparison between HEDs and chondrites effectively eliminates a source of analytical

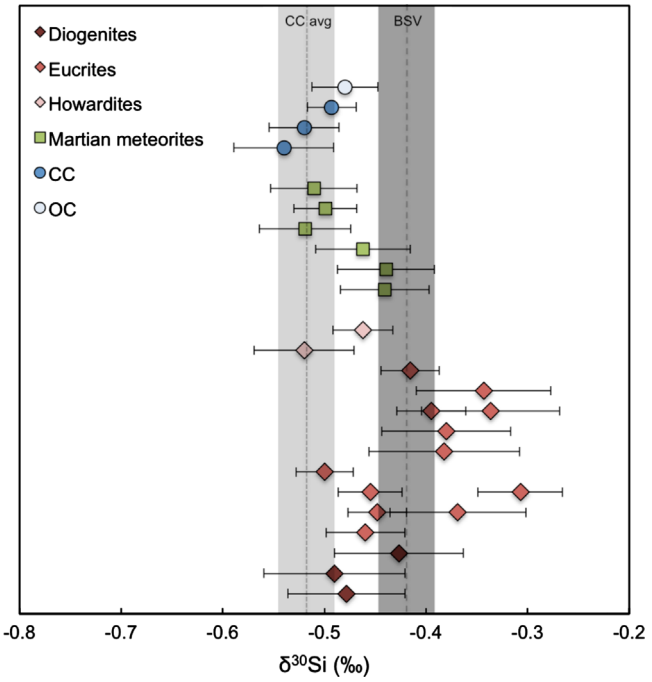

Fig. 2. Silicon isotope data for chondrites, Martian meteorites and HED meteorites relative to the bracketing standard NBS28 (error bars are two standard error). The dotted line and light gray box represent the carbonaceous chondrite average (± 2 se). The dashed line and dark gray box represent the Si isotopic composition of Bulk Silicate Vesta (BSV), calculated as the eucrite and diogenite average (± 2 se).

error, making non-zero isotopic offsets easier to resolve; when comparing data bracketed using the traditional NBS28 international Si isotopic standard, the uncertainty is compounded because the error is propagated. Since this is a non-traditional analytical approach, two different chondrites (Cold Bokkeveld and Allende) are used to ensure the method is robust and the data obtained are consistent regardless of the specific bracketing chondrite.

As a check for accuracy, NBS28, BHVO-2 and other chondrites (e.g. the CM2 Murray) were also processed through chemistry and measured against carbonaceous chondrites. When bracketed by Cold Bokkeveld, the average values for NBS28 and BHVO-2 are $\delta^{30}Si_{CB}=0.59\pm0.02$‰ and $\delta^{30}Si_{CB}=0.22\pm0.02$‰ respectively; these values are in agreement with the relative values obtained by NBS28 bracketing. The Si isotopic compositions of the carbonaceous chondrites Allende and Murray are not resolvable from Cold Bokkeveld, with an average value of $\delta^{30}Si_{CB}=-0.02\pm0.06$‰. The Martian meteorite data (average $\delta^{30}Si_{CB}=0.05\pm0.05$‰) are also indistinct from the chondrite bracketing standard.

In contrast, the Si isotope compositions of both eucrites and diogenites are distinctly heavy with respect to carbonaceous chondrites. When bracketed by Cold Bokkeveld, the eucrite average is $\delta^{30}Si_{CB}=0.13\pm0.04$‰ and the diogenite average is $\delta^{30}Si_{CB}=0.11\pm0.11$‰. Allende was also used as the bracketing standard during a separate analytical session, yielding similar results for both eucrites (average $\delta^{30}Si_{Allende}=0.12\pm0.03$‰) and diogenites (average $\delta^{30}Si_{Allende}=0.16\pm0.06$‰). The combined averages for eucrites and diogenites are $\delta^{30}Si_{CB}=0.12\pm0.05$‰ and $\delta^{30}Si_{Allende}=0.13\pm0.03$‰.

4. Discussion

4.1. Quantifying the Si isotopic offset between HEDs and chondrites

This study is the first to note a resolvable difference in Si isotope composition between Bulk Silicate 4-Vesta (BSV) and carbonaceous chondrites. Although there was a hint of this in previous studies (Armytage et al., 2011; Zambardi, 2011), prior data were not able to resolve a difference within analytical error. Relative to the traditional Si isotope bracketing standard NBS28, we find the difference between BSV and carbonaceous chondrites (CC) to be $\Delta^{30}Si_{BSV\text{-}CC}=0.10\pm0.06$‰ (1 standard deviation), where $\Delta^{30}Si_{BSV\text{-}CC}=\delta^{30}Si$ (BSV)$-\delta^{30}Si$ (carbonaceous chondrites).

In order to validate these results, representative samples of HED meteorites, carbonaceous chondrites and Martian meteorites were measured using carbonaceous chondrites as bracketing standards. The chondrite bracketed Si isotope data are in very good agreement with the data measured against NBS28 for both standards and meteorite samples. For example, when bracketed by NBS28, the terrestrial basalt standard BHVO-2 ($\delta^{30}Si=-0.28\pm0.02$‰) is 0.24 per mil heavier than carbonaceous chondrites ($\delta^{30}Si=-0.52\pm0.03$‰), which is in good agreement with the data for BHVO-2 when bracketed by Cold Bokkeveld ($\delta^{30}Si_{CB}=0.22\pm0.02$‰). Similarly, on average the $^{30}Si/^{28}Si$ ratios of eucrites and diogenites are consistently ~0.1‰ heavier than chondrites when bracketed by either NBS28 or by a carbonaceous chondrite. Furthermore, when considered on an individual basis, the Si isotopic composition of all HED meteorites measured are heavier than the bracketing chondrite, and the difference in all but one HED is resolvable within 2 se. Therefore, we believe that there is a distinct difference between the Si isotopic composition of BSV and carbonaceous chondrites. For subsequent calculations, the offset calculated from bracketing by NBS28, $\Delta^{30}Si_{BSV\text{-}CC}=0.10\pm0.06$‰ (1 sd), is used to quantify this difference. We will now examine the possible interpretations of the Si isotope offset between BSV and carbonaceous chondrites.

4.2. Assessing the possible causes of the heavy Si isotope enrichment in HEDs

Igneous processes are a possible source of Si isotope fractionation in HED meteorites, as has been observed for Fe isotopes (Wang et al., 2012). This is an unlikely explanation for the $\delta^{30}Si$ offset observed in HEDs since no isotopic fractionation has been found in terrestrial or Martian basalts (Savage et al., 2010; Armytage et al., 2011). If magmatic differentiation was the cause of the heavy Si isotope enrichment in HEDs, eucrites should be isotopically heavier than diogenites (Savage et al., 2011). However, although they have different igneous origins, both diogenites and eucrites have similar isotopic compositions as is especially evident in the chondrite-bracketed data (see Table 2 and Fig. 3). Therefore, this suggests that igneous processes do not account for the Si isotope fractionation found in HEDs, and the Si isotopic composition recorded in HED meteorites is representative of BSV.

Isotopic fractionation associated with evaporation is a mechanism that could potentially fractionate Si isotopes (e.g. Pahlevan et al., 2011). During evaporation, lighter isotopes are preferentially incorporated into the vapor phase, resulting in an isotopically heavy residue. This volatile loss is proportional to the volatility of an element and two elements with similar volatilities should show similar isotopic fractionation. However, no isotopic fractionation has been observed in HED meteorites for elements with volatilities similar to Si. Silicon has a 50% condensation temperature (T_c) of 1310 K, which is comparable to Fe (50% $T_c=1334$ K) and Mg (50% $T_c=1336$ K; Lodders, 2003). Neither Fe (Poitrasson et al., 2004; Wang et al., 2012) nor Mg (Wiechert and Halliday, 2007) shows isotopic variation between HED meteorites and chondrites consistent with evaporation. In addition, Li (50% $T_c=1142$ K), an element that is more volatile than Si, does not display isotopic variability due to evaporative processes in HED meteorites (Seitz et al., 2007). Finally, although the Moon is depleted in volatile elements relative to Earth, the average Si isotopic composition

Table 2
Silicon isotope data for standards and meteorite samples relative to the carbonaceous chondrites Cold Bokkeveld and Allende as bracketing standards.

Sample	$\delta^{29}Si_{CB}$ [a]	2 sd [b]	2se [c]	$\delta^{30}Si_{CB}$	2 sd	2 se	n [d]	$\delta^{29}Si_{Allende}$ [e]	2 sd	2 se	$\delta^{30}Si_{Allende}$ [e]	2 sd	2 se	n
NBS28	0.30	0.03	0.01	0.59	0.07	0.02	11							
BHVO-2	0.11	0.06	0.02	0.22	0.06	0.02	8							
Carbonaceous chondrites														
Allende	0.01	0.06	0.02	0.01	0.09	0.03	12							
Murray	−0.04	0.03	0.01	−0.05	0.05	0.02	6							
Average-carbonaceous chondrites	**−0.02**	**0.07**	**0.05**	**−0.02**	**0.09**	**0.06**	**2**							
Martian meteorites														
Sayh al Uhaymir 008	0.03	0.06	0.03	0.08	0.04	0.02	4							
Los Angeles	0.04	0.09	0.04	0.08	0.08	0.04	4							
Miller Range 03346	0.03	0.09	0.04	0.01	0.12	0.05	5							
Average-Martian meteorites	**0.03**	**0.02**	**0.01**	**0.05**	**0.09**	**0.05**	**3**							
HED meteorites														
Eucrites														
Serra de Magé	0.06	0.06	0.02	0.10	0.10	0.04	6	0.06	0.05	0.02	0.11	0.07	0.03	6
Cachari #1	0.12	0.06	0.02	0.19	0.18	0.05	12	0.10	0.05	0.04	0.16	0.08	0.03	6
Juvinas	0.06	0.02	0.01	0.12	0.08	0.03	6	0.03	0.05	0.01	0.09	0.06	0.03	6
#1	0.07	0.04	0.01	0.11	0.10	0.03	10	0.05	0.05	0.02	0.11	0.03	0.01	6
Average-Eucrites	**0.08**	**0.05**	**0.03**	**0.13**	**0.08**	**0.04**	**4**	**0.06**	**0.06**	**0.03**	**0.12**	**0.07**	**0.03**	**4**
Diogenites														
Aioun el Atrouss	0.10	0.03	0.01	0.20	0.08	0.03	6	0.09	0.01	0.04	0.19	0.09	0.04	6
Tatahouine	0.08	0.05	0.02	0.13	0.06	0.03	6	0.06	0.04	0.03	0.13	0.09	0.04	6
Shalka	0.02	0.07	0.03	0.01	0.12	0.05	5							
Average-diogenites	**0.07**	**0.08**	**0.05**	**0.11**	**0.20**	**0.11**	**3**	**0.07**	**0.04**	**0.05**	**0.16**	**0.08**	**0.06**	**2**
Average-eucrites and diogenites	**0.07**	**0.06**	**0.02**	**0.12**	**0.13**	**0.05**	**7**	**0.07**	**0.05**	**0.03**	**0.13**	**0.08**	**0.03**	**6**

[a] $\delta^{29}Si_{CB}$ and $\delta^{30}Si_{CB}$ are the Si isotope data relative to Cold Bokkeveld as the bracketing standard.
[b] 2 sd = 2 × standard deviation.
[c] 2 se = 2 × standard deviation/$\sqrt{n}$.
[d] n = number of measurements.
[e] $\delta^{29}Si_{Allende}$ and $\delta^{30}Si_{Allende}$ are the Si isotope data relative to Allende as the bracketing standard.

of lunar samples is identical to the composition of the BSE (Chakrabarti and Jacobsen, 2010; Armytage et al., 2012; Fitoussi and Bourdon, 2012). Therefore, evaporation is an unlikely explanation for the difference between BSV and carbonaceous chondrites in Si isotopes.

Theoretical calculations (Georg et al., 2007), metal-silicate partitioning experiments (Shahar et al., 2009, 2011; Ziegler et al., 2010), and empirical measurements (Ziegler et al., 2010; Savage and Moynier, 2013) show that Si isotopes are fractionated during metal–silicate equilibrium reactions, with the silicate enriched in the heavier isotopes compared to the metal. These results, combined with the observation that the BSE is enriched in the heavier isotopes of Si compared to chondrites, have been used as an argument for Si as a light element in Earth's core.

The heavier Si isotopic composition of BSV compared to carbonaceous chondrites is evidence for the incorporation of Si into 4-Vesta's core. In contrast, the absence of resolvable isotopic fractionation between Martian meteorites and chondrites is consistent with the absence of Si in the core of Mars. Based on the measurement of Si isotope ratios in HED meteorites, and assuming that the Si isotopic composition of bulk 4-Vesta is chondritic, the amount of Si present in 4-Vesta's core can be estimated using simple mass balance (Eq. (1)):

$$\Delta^{30}Si_{BSV-CC} = \varepsilon f_{core} \quad (1)$$

where f_{core} is the mass fraction of Si in 4-Vesta's core and ε is the metal–silicate fractionation factor. For these calculations, we use $\varepsilon = 7.45 \pm 0.41 \times 10^6/T^2$ as estimated by Shahar et al. (2011) and 1800–2000 K as the range of possible temperatures during 4-Vesta's core formation (Righter and Drake, 1996, 1997). The results of these calculations are presented in Table 3. For example, at a temperature of 1800 K and using the conservative minimum value of $\Delta^{30}Si_{BSV-CC} = 0.04$, the calculated amount of Si in 4-Vesta's core is 1 wt% when the elemental abundance of Si in 4-Vesta is considered to be equal to that of CI chondrites (10 wt% Si) and is 1.7 wt% when the elemental abundance of Si in 4-Vesta is considered to be equal to that of LL chondrites (18 wt% Si). CI chondrites and LL chondrites are used as compositional end-members of the possible precursor chondritic material that accreted to form 4-Vesta. These results represent the first evidence of Si partitioning into 4-Vesta's core and have important implications for our knowledge of the conditions of core formation, particularly oxygen fugacity.

4.3. Redox conditions during core formation on 4-Vesta

The reaction describing Si partitioning between metal and silicate is

$$2Fe_{metal} + SiO_{2silicate} = 2FeO_{silicate} + Si_{metal} \quad (2)$$

The equilibrium constant for this reaction, K_{Si}, can be modeled as a function of pressure, temperature and chemical composition using Eq. (3) (see Wade and Wood, 2005; Ricolleau et al., 2011; or Siebert et al., 2012 for details):

$$\log K_{Si} = a + \frac{b}{T} + \frac{cP}{T} + d\frac{nbo}{t} \quad (3)$$

where a, b, c, and d are regression constants, T is the temperature in K, P is the pressure in GPa (fixed at 4-Vesta's core boundary pressure of 0.1 GPa), and nbo/t is the molar ratio of non-bridging oxygen per tetrahedrally coordinated cations in the silicate melt, which is calculated from the CI chondrite and LL chondrite bulk composition models for 4-Vesta (Righter and Drake, 1997). The constants a, b, c and d (−1.27, −11,396 K, 98 K/GPa and 0.236,

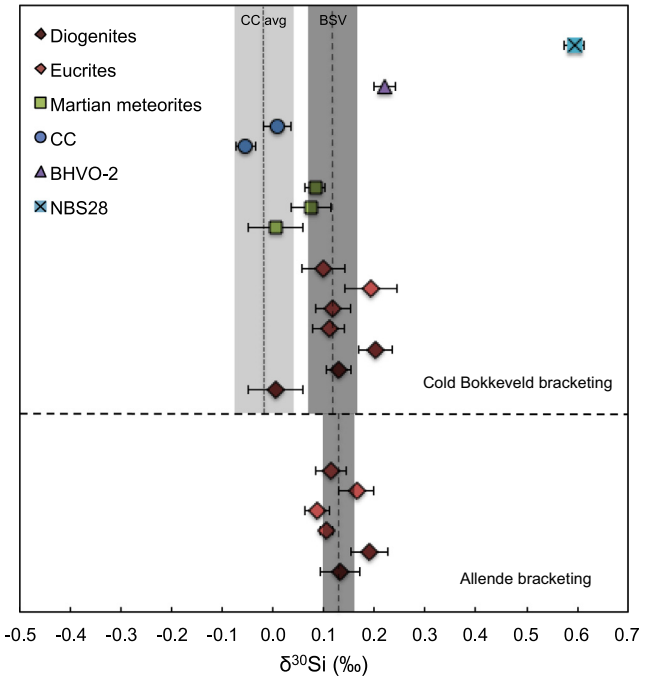

Fig. 3. Silicon isotope data for terrestrial standards, chondrites, Martian meteorites and HED meteorites relative to the carbonaceous chondrites Cold Bokkeveld and Allende as bracketing standards (error bars are 2 se). The dotted line and light gray box represent the carbonaceous chondrite average with respect to Cold Bokkeveld (± 2 se). The dashed lines and dark gray boxes represent the Si isotopic composition of Bulk Silicate Vesta (BSV) relative to Cold Bokkeveld and Allende, calculated as the eucrite and diogenite averages (± 2 se).

Table 3
Calculated wt% Si in 4-Vesta's core at possible core boundary temperatures. 4-Vesta's core mass fraction is considered to be 0.18 of its total mass (Russell et al., 2012).

T (K)	ε[a]	$\Delta^{30}Si_{BSV-CC}$ (‰)	f_{core}[b]	Si[c] (wt%)	Si[d] (wt%)
1800	2.30	0.04	0.017	1.0	1.7
2000	1.86	0.04	0.021	1.2	2.1

[a] ε is the metal–silicate fractionation factor, as given by Shahar et al. (2011).
[b] Calculated fraction of Si in Vesta's core.
[c] Calculated wt% Si of 4-Vesta's core assuming 4-Vesta has CI chondrite composition (10 wt% Si).
[d] Calculated wt% Si of 4-Vesta's core assuming 4-Vesta has LL chondrite composition (18 wt% Si).

respectively) are obtained from a least-squares linear regression of previously published Si metal silicate partitioning data (Ito et al., 1995; Kilburn and Wood, 1997; Gessmann and Rubie, 1998; Wade and Wood, 2001; Malavergne et al., 2007; Corgne et al., 2008; Mann et al., 2009; Ricolleau et al., 2011).

In addition, $\log K_{Si}$ can be expressed as

$$\log K_{Si} = \log\frac{X_{Si}^{metal}}{X_{SiO_2}^{silicate}} + 2\log\frac{X_{FeO}^{silicate}}{X_{Fe}^{metal}} + \log\frac{\gamma_{Si}^{metal}}{(\gamma_{Fe}^{metal})^2} + \log\frac{(\gamma_{FeO}^{silicate})^2}{\gamma_{SiO_2}^{silicate}} \quad (4)$$

where X_j^i (and γ_j^i) are the molar fraction (and activity coefficient) of element or molecule j (Fe, FeO, Si, SiO_2) in phase i (metal or silicate). The CI chondrite and LL chondrite composition models of Righter and Drake (1997) are used for the SiO_2 fraction of BSV, γ_{Fe}^{metal} is calculated according to the formalism developed by Ma, 2001 (see Corgne et al., 2009), and γ_{Si}^{metal} is taken from Schlesinger and Xiang (2001). Finally, the last term (ratio of activity coefficients in the silicate phase) in Eq. (4) is set equal to zero, since this effect is empirically taken into account in the $d \times nbo/t$ parameter in Eq. (3).

By combining Eqs. (3) and (4), it is possible to calculate the concentration of Si in the metal phase as a function of oxygen fugacity, which is expressed as the deviation from the iron–wüstite buffer, $\Delta IW = 2\log_{10}(X_{FeO}^{silicate}/X_{Fe}^{metal})$, for various temperatures (see Eq. (5) and Fig. 4).

$$\log X_{Si}^{metal} = a + \frac{b}{T} + \frac{cP}{T} + d\frac{nbo}{t} - \log X_{SiO_2}^{silicate} - \Delta IW - \log\frac{\gamma_{Si}^{metal}}{(\gamma_{Fe}^{metal})^2} \quad (5)$$

In order to have a Si concentration of ~1 wt% in 4-Vesta's core, these calculations require that the oxygen fugacity (fO_2) during core formation was $-4.3 < \Delta IW < -4.1$. This is lower than the fO_2 value ($\Delta IW \sim -1$) estimated for the time of formation of the eucrites, which corresponds to the silicate differentiation of BSV following core formation (Stolper, 1977). This suggests that 4-Vesta accreted under relatively reducing conditions, intermediary between conditions during enstatite chondrite formation ($\Delta IW \sim -5$) and terrestrial accretion ($\Delta IW \sim -2.5$), and within a

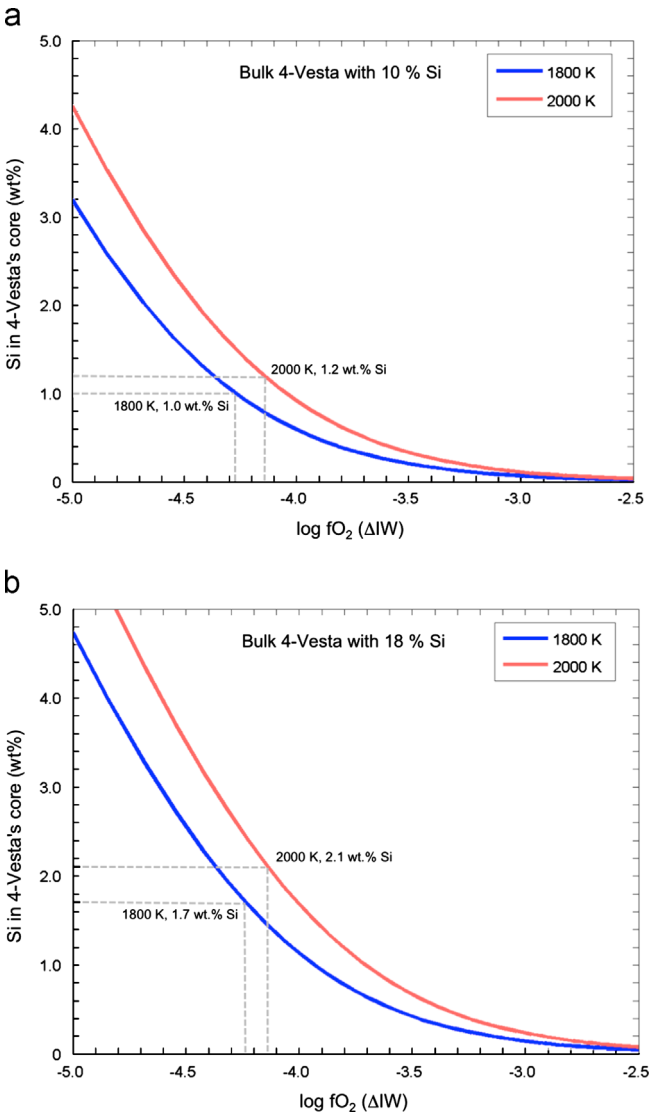

Fig. 4. Modeled Si content in the core of 4-Vesta as a function of fO_2 relative to the IW buffer for core formation temperatures of 1800 K and 2000 K with elemental Si abundances in 4-Vesta modeled as (a) CI chondrite composition (10 wt% Si) and (b) LL chondrite composition (18 wt% Si). The dashed gray tie-lines represent wt% of Si in 4-Vesta's core and the corresponding fO_2 required by Eq. (5) for each temperature curve.

few million years the fO_2 of BSV increased by ~3ΔIW log units. This scenario satisfies current planetary formation models (e.g. Walsh et al., 2011) involving an inward then outward migration of materials very early in Solar System history. Our results suggest that 4-Vesta accreted from reduced volatile-poor materials much closer to the Sun and later moved outwards to its present location. Late accretion of more oxidized materials along with self-oxidation of BSV as a consequence of Si migrating into the core (Wade and Wood, 2005) could explain the increase in the fO_2 of BSV and would also explain the over-abundance of highly siderophile elements present in diogenites (Day et al., 2012).

Finally, the discrepancy between the oxygen fugacity during 4-Vesta's core formation estimated from the Si isotopic composition of BSV (ΔIW~−4) and from moderately siderophile element (MSE) partitioning (ΔIW~−2; Righter and Drake, 1997) requires explanation. Based on the abundances of highly siderophile elements measured in diogenites, it has been recently proposed that up to 0.5–1.5% of 4-Vesta's mass comes from late-accreted (post–core formation) chondritic material (Day et al., 2012). Day et al. (2012) did not measure MSE abundances in HEDs, but the addition of chondritic material after core formation would certainly enrich 4-Vesta in such elements; in contrast, the addition of a small amount of chondritic Si would not significantly affect the Si isotopic composition of BSV. To determine the effect of core formation on MSE abundances in the silicate portion of 4-Vesta, the late-accreted chondritic component must be subtracted from the current models of MSE abundances in BSV. Hence the effective metal–silicate partition coefficients for MSEs during core formation on 4-Vesta is necessarily higher than previously thought. This natural increase in the effective metal–silicate partition coefficients of MSEs implies that these elements partitioned more strongly into 4-Vesta's core, and therefore the fO_2 at the time of core formation was necessarily lower than the fO_2 obtained without taking into account the MSE contribution from late-accretion. The exact magnitude of this correction depends on the mass of late-accreted material, which has still to be estimated through high-precision measurements of MSE abundances in eucrites and diogenites.

5. Conclusions

There is a resolvable Si isotope difference between HED meteorites and chondrites. The HED meteorite data are distinctly heavier than carbonaceous chondrites, with an average difference of $\Delta^{30}Si_{BSV\text{-}CC} = 0.10 \pm 0.06‰$ (1 sd). Incorporation of Si as a light element into 4-Vesta's core is the most likely explanation for the heavier Si isotopic composition of HED meteorites. Based on these data, 4-Vesta's core contains ~1 wt% Si. In agreement with previous studies, we find that the Martian meteorite Si isotope data are not resolvable from chondrites, suggesting the absence of Si in Mars' core.

The incorporation of Si into 4-Vesta's core has implications for the conditions prevalent during core formation, particularly oxygen fugacity. Thermodynamic calculations indicate an oxygen fugacity during 4-Vesta's core formation of $-4.3 < \Delta IW < -4.1$, which is lower than the redox state previously calculated for HED meteorite formation. These results imply that 4-Vesta accreted and differentiated a core under relatively reducing conditions and subsequently accreted a late veneer of chondritic material.

This work illustrates the important potential of Si isotopes as tracers of core formation processes in differentiated planetary bodies. As more remote sensing data is acquired on a wider range of asteroids, and the parent bodies of additional achondrite meteorite samples are identified, future work on the redox conditions prevalent during core formation in asteroids will be possible.

Acknowledgments

Insightful comments by Editor Bernard Marty and two anonymous reviewers greatly improved the quality of the manuscript. We thank Julien Foriel for maintaining the MC-ICP-MS and the clean lab facilities at Washington University in St. Louis and Bruce Fegley for insightful discussion. This work was made possible by the provision of samples from Timothy McCoy (US National Museum of Natural History, Smithsonian Institution, Washington, DC), Alex Bevan (Western Australian Museum, Perth), Franz Brandstatter (Naturhistorisches Museum, Vienna), James Holstein, Clarita Nunez and Philip Heck (The Field Museum, Chicago), Meenakshi Wadhwa (Arizona State University, Tempe), Cecilia Satterwhite (NASA Johnson Space Center, Houston) and the Comite de Gestion (Museum Nationale d'Histoire Naturelle, Paris) and Guy Consolmagno (Vatican). This work was supported by the NASA EXO (NNX12AD88G) and the COSMO (NNX12AH70G) grants to FM. EP and PS thank the McDonnell Center for Space Sciences for funding.

References

Abraham, K., Opfergelt, S., Fripiat, F., Cavagna, A., de Jong, J.T.M., Foley, S.F., André, L., Cardinal, D., 2008. $\delta^{30}Si$ and $\delta^{29}Si$ determinations on USGS BHVO-1 and BHVO-2 reference materials with a new configuration on a Nu plasma multi-collector ICP-MS. Geostand. Geoanal. Res. 32, 193–202.

Allègre, C.J., Poirier, J.P., Humler, E., Hofman, A., 1995. The chemical composition of the Earth. Earth Planet. Sci. Lett. 134, 515–526.

Antonangeli, D., Siebert, J., Badro, J., Farber, D.L., Fiquet, G., Morard, G., Ryerson, F.J., 2010. Composition of the Earth's inner core from high-pressure sound velocity measurements in Fe–Ni–Si alloys. Earth Planet. Sci. Lett. 295, 292–296.

Armytage, R.M.G., Georg, R.B., Savage, P.S., Williams, H.M., Halliday, A.N., 2011. Silicon isotopes in meteorites and planetary core formation. Geochim. Cosmochim. Acta 75, 3662–3676.

Armytage, R.M.G., Georg, R.B., Williams, H.M., Halliday, A.N., 2012. Silicon isotopes in lunar rocks: implications for the Moon's formation and the early history of the Earth. Geochim. Cosmochim. Acta 77, 504–514.

Badro, J., Fiquet, G., Guyot, F., Gregoryanz, E., Occelli, F., Antonangeli, D., d'Astuto, M., 2007. Effect of light elements on the sound velocities in solid iron: implications for the composition of Earth's core. Earth Planet. Sci. Lett. 254, 233–238.

Barrat, J.A., Yamaguchi, A., Zanda, B., Bollinger, C., Bohn, M., 2010. Relative chronology of crust formation on asteroid Vesta: insights from the geochemistry of diogenites. Geochim. Cosmochim. Acta 74, 6218–6231.

Birch, F., 1964. Density and composition of mantle and core. J. Geophys. Res. 69 (20), 4377–4388.

Chakrabarti, R., Jacobsen, S.B., 2010. Silicon isotopes in the inner solar system: implications for core formation, solar nebular processes and partial melting. Geochim. Cosmochim. Acta 74, 6921–6933.

Corgne, A., Keshav, S., Wood, B.J., McDonough, W.F., Fei, Y., 2008. Metal–silicate partitioning and constraints on core composition and oxygen fugacity during Earth accretion. Geochim. Cosmochim. Acta 72, 574–589.

Corgne, A., Siebert, J., Badro, J., 2009. Oxygen as a light element: a solution to single-stage core formation. Earth Planet. Sci. Lett. 288, 108–114.

Day, J.M.D., Walker, R.J., Qin, L., Rumble III, D., 2012. Late accretion as a natural consequence of planetary growth. Nat. Geosci. 5, 614–617.

De Sanctis, M.C., Ammannito, E., Capria, M.T., Tosi, F., Capaccioni, F., Zambon, F., Carraro, F., Fonte, S., Frigeri, A., Jaumann, R., Magni, G., Marchi, S., McCord, T.B., McFadden, L.A., McSween Jr., H.Y., Mittlefehldt, D.W., Nathues, A., Palomba, E., Pieters, C.M., Raymond, C.A., Russell, C.T., Toplis, M.J., Turrini, D., 2012. Spectroscopic characterization of mineralogy and its diversity across Vesta. Science 336, 697–700.

Fitoussi, C., Bourdon, B., 2012. Silicon isotope evidence against an enstatite chondrite earth. Science 335, 1477–1480.

Fitoussi, C., Bourdon, B., Kleine, T., Oberli, F., Reynolds, B.C., 2009. Si isotope systematics of meteorites and terrestrial peridotites: implications for Mg/Si fractionation in the solar nebula and for Si in the Earth's core. Earth Planet. Sci. Lett. 287, 77–85.

Georg, R.B., Halliday, A.N., Schauble, E.A., Reynolds, B.C., 2007. Silicon in the Earth's core. Nature 447, 1102–1106.

Georg, R.B., Reynolds, B.C., Frank, M., Halliday, A.N., 2006. New sample preparation techniques for the determination of Si isotopic compositions using MC-ICPMS. Chem. Geol. 235, 95–104.

Gessmann, C.K., Rubie, D.C., 1998. The effect of temperature on the partitioning of nickel, cobalt, manganese, chromium, and vanadium at 9 GPa and constraints on formation of the Earth's core. Geochim. Cosmochim. Acta 62, 867–882.

Gessmann, C.K., Wood, B.J., Rubie, D.C., Kilburn, M.R., 2001. Solubility of silicon in liquid metal at high pressure: implications for the composition of the Earth's core. Earth Planet. Sci. Lett. 184, 367–376.
Ito, E., Morooka, K., Ujike, O., Katsura, T., 1995. Reactions between molten iron and silicate melts at high pressure: implications for the chemical evolution of Earth's core. J. Geophys. Res. 100, 5901–5910.
Janots, E., Gnos, E., Hofmann, A.W., Greenwood, R.C., Franchi, I.A., Bermingham, K., Netwing, V., 2012. Jiddat al Harasis 556: a howardite impact melt breccia with an H chondrite component. Meteorit. Planet. Sci. 47, 1558–1574.
Kempl, J., Vroon, P.Z., Zinngrebe, E., van Westrenen, W., 2013. Si isotope fractionation between Si-poor metal and silicate melt at pressure–temperature conditions relevant to metal segregation in small planetary bodies. Earth Planet. Sci. Lett. 368, 61–68.
Kilburn, M.R., Wood, B.J., 1997. Metal–silicate partitioning and the incompatibility of S and Si during core formation. Earth Planet. Sci. Lett. 152, 139–148.
Lodders, K., 2003. Solar system abundances and condensation temperatures of the elements. Astrophys. J. 591, 1220–1247.
Ma, Z., 2001. Thermodynamic description for concentrated metallic solutions using interaction parameters. Metall. Mater. Trans. B 32, 87–103.
Malavergne, V., Tarrida, M., Combes, R., Bureau, H., Jones, J., Schwandt, C., 2007. New high-pressure and high-temperature metal/silicate partitioning of U and Pb: implication for the cores of the Earth and Mars. Geochim. Cosmochim. Acta 71, 2637–2655.
Mann, U., Frost, D.J., Rubie, D.C., 2009. Evidence for high-pressure core mantle differentiation from the metal–silicate partitioning of lithophile and weakly-siderophile elements. Geochim. Cosmochim. Acta 73, 7360–7386.
McDonough, W.F., 2003. Compositional model for the Earth's core. In: Carlson, R. (Ed.), The Mantle and Core. In: Holland, Heinrich D., Turekian, Karl K. (Eds.), Treatise on Geochemistry, vol. 2. Elsevier-Pergamon, Oxford, pp. 547–568.
Moynier, F., Yin, Q.-Z., Schauble, E.A., 2011. Isotopic evidence of Cr partitioning into Earth's core. Science 331, 1417–1420.
Pahlevan, K., Stevenson, D.J., Eiler, J.M., 2011. Chemical fractionation in the silicate vapor atmosphere of the Earth. Earth Planet. Sci. Lett. 301, 433–443.
Poitrasson, F., Halliday, A.N., Lee, D.-C., Levasseur, S., Teutsch, N., 2004. Iron isotope differences between Earth, Moon, Mars and Vesta as possible records of contrasted accretion mechanisms. Earth Planet. Sci. Lett. 223, 253–266.
Ricolleau, A., Fei, Y.W., Corgne, A., Siebert, J., Badro, J., 2011. Constraints on oxygen and silicon contents of Earth's core from metal–silicate partitioning experiments at high pressure and temperature. Earth Planet. Sci. Lett. 310, 409–421.
Righter, K., Drake, M.J., 1996. Core formation in Earth's moon, Mars, and Vesta. Icarus 124, 513–529.
Righter, K., Drake, M.J., 1997. A magma ocean on Vesta: core formation and petrogenesis of eucrites and diogenites. Meteorit. Planet. Sci. 32, 929–944.
Russell, C.T., Raymond, C.A., Coradini, A., McSween Jr., H.Y., Zuber., M.T., Nathues, A., De Sanctis, M.C., Jaumann, R., Konopliv, A.S., Preusker, F., Asmar, S.W., Park, R.S., Gaskell, R., Keller, H.U., Mottola, S., Roatsch, T., Scully, J.E.C., Smith, D.E., Tricarico, P., Toplis, M.J., Christensen, U.R., Feldman, W.C., Lawrence, D.J., McCoy, T.J., Prettyman, T.H., Reedy, R.C., Sykes, M.E., Titus, T.N., 2012. Dawn at Vesta: testing the protoplanetary paradigm. Science 336, 684–686.
Savage, P.S., Georg, R.B., Armytage, R.M.G., Williams, H.M., Halliday, A.N., 2010. Silicon isotope homogeneity in the mantle. Earth Planet. Sci. Lett. 295, 139–146.
Savage, P.S., Georg, R.B., Williams, H.M., Burton, K.W., Halliday, A.N., 2011. Silicon isotope fractionation during magmatic differentiation. Geochim. Cosmochim. Acta 75, 6124–6139.
Savage, P.S., Moynier, F., 2013. Silicon isotopic variation in enstatite meteorites: clues to their origin and Earth-forming material. Earth Planet. Sci. Lett. 361, 487–496.
Schlesinger, M.E., Xiang, Q., 2001. Enthalpies of mixing in Fe–C–Si melts. J. Alloys Compd. 321, 242–247.
Seitz, H.M., Brey, G.P., Zipfel, J., Ott, U., Weyer, S., Durali, S., Weinbruch, S., 2007. Lithium isotope composition of ordinary and carbonaceous chondrites, and differentiated planetary bodies: bulk solar system and solar reservoirs. Earth Planet. Sci. Lett. 260, 582–596.
Shahar, A., Hillgren, V.J., Young, E.D., Fei, Y., Macris, C.A., Deng, L., 2011. High-temperature Si isotope fractionation between iron metal and silicate. Geochim. Cosmochim. Acta 75, 7688–7697.
Shahar, A., Ziegler, K., Young, E.D., Ricolleau, A., Schauble, E.A., Fei, Y., 2009. Experimentally determined Si isotope fractionation between silicate and Fe metal and implications for Earth's core formation. Earth Planet. Sci. Lett. 288, 228–234.
Siebert, J., Badro, J., Antonangeli, D., Ryerson, F.J., 2012. Metal–silicate partitioning of Ni and Co in a deep magma ocean. Earth Planet. Sci. Lett. 321–322, 189–197.
Stolper, E., 1977. Experimental petrology of eucritic meteorites. Geochim. Cosmochim. Acta 41, 587–611.
Trinquier, A., Birck, J.-L., Allégre, C.J., Gopel, C., Ulfbeck, D., 2008. ^{53}Mn–^{53}Cr systematics of the early Solar System revisited. Geochim. Cosmochim. Acta 72, 5146–5163.
Wade, J., Wood, B.J., 2001. The Earth's missing niobium may be in the core. Nature 409, 75–78.
Wade, J., Wood, B.J., 2005. Core formation and the oxidation state of the Earth. Earth Planet. Sci. Lett. 236, 78–95.
Walsh, K.J., Morbidelli, A., Raymond, S.N., O'Brien, D.P., Mandell, A.M., 2011. A low mass for Mars from Jupiter's early gas-driven migration. Nature 475, 206–209.
Wang, K., Moynier, F., Dauphas, N., Barrat, J.-A., Craddock, P., Sio, C.K., 2012. Iron isotope fractionation in planetary crusts. Geochim. Cosmochim. Acta 89, 31–45.
Wiechert, U., Halliday, A.N., 2007. Non-chondritic magnesium and the origins of the inner terrestrial planets. Earth Planet. Sci. Lett. 256, 360–371.
Zambardi, T., 2011. Recherche de marqueurs de processus de formation des planètes à travers les isotopes stables de masse moyenne (Ph.D. thesis). Université Paul Sabatier, Toulouse III, 214 pp.
Ziegler, K., Young, E.D., Schauble, E.A., Wasson, J.T., 2010. Metal–silicate silicon isotope fractionation in enstatite meteorites and constraints on Earth's core formation. Earth Planet. Sci. Lett. 295, 487–496.